Adaptive Quantum Nondemolition Measurement of a Photon Number

B. Peaudecerf,[1] T. Rybarczyk,[1] S. Gerlich,[1] S. Gleyzes,[1] J. M. Raimond,[1] S. Haroche,[1,2] I. Dotsenko,[1,2,*] and M. Brune[1,2]
[1]*Laboratoire Kastler Brossel, ENS, UPMC-Paris 6, CNRS, Collège de France, 24 rue Lhomond, 75005 Paris, France*
[2]*Collège de France, 11 place Marcelin Berthelot, 75005 Paris, France*
(Received 25 September 2013; published 26 February 2014)

In many quantum measurements, information is acquired incrementally by the successive interaction of meters with the measured system. Adaptive measurements minimize the use of resources (meters) by adjusting the measurement settings according to available information. We demonstrate an adaptive measurement for nondestructive photon counting in a cavity, based on Ramsey interferometry for Rydberg atoms interacting with the field. Tuning the interferometer in real time, we speed up the measurement by up to 45%. Such adaptive methods are promising for quantum metrology, state preparation, and feedback.

DOI: 10.1103/PhysRevLett.112.080401 PACS numbers: 03.65.Wj, 03.65.Ta, 42.50.Dv, 42.50.Pq

Quantum measurement, which takes place at the interface between the quantum world and the macroscopic reality, plays an essential role in quantum metrology, quantum information, and quantum communication. Among all measurement strategies, the quantum nondemolition (QND) ones are of particular interest [1]. They implement the ideal repeatable projective measurement described by the basic postulates, allowing us to follow in real time the system's evolution as a series of quantum jumps between the measurement eigenstates. They open the door to high-sensitivity detection of minute perturbations.

QND measurements have been realized in a few contexts [2,3], including the measurement of the intensity of a macroscopic laser beam, the collective spin of an atomic ensemble [4], and the counting of photons stored in a cavity [5]. These measurements are performed indirectly by coupling the system to quantum meters, whose states are finally measured. For laser beams and spin ensembles, the meters are photons, finally destructively counted. For photons in cavities, the meters are atoms, interacting dispersively with the field.

In principle, one meter system would be sufficient, provided its Hilbert space is at least as large as that of the measured system. It is generally not the case. In the QND photon counting, meters are two-level atoms which interact successively with the field and whose detection provides binary information. The measurement gathers information from many meters, resulting in a progressive collapse of the field state, which should occur on a time scale smaller than that of the system's decoherence. It is thus important to reduce the amount of resources (meters) required and to approach the minimum determined by information theory.

Adaptive measurement strategies aim to achieve this resource reduction by adapting, for each meter, the parameters of its interaction with the system and/or the settings of its detection, according to all information available at the time [6]. Measurements realizing part or all of these objectives have already been reported [7–9]. Most relied on absorptive detection of light [7,10] for an optimized estimation of the optical phase of propagating light fields. These experiments are particularly relevant for practical applications to quantum-enabled metrology and continuous-variable quantum communication. However, none so far has tackled the adaptive QND detection of photons. It is of great importance for microwave cavity quantum electrodynamics (QED) [5], but also in the thriving field of circuit QED [11] and for optical cavity QED, in which QND detection of photons has been recently reported [12], with considerable possible impact for quantum communication.

We report here the adaptive QND counting of the number n of photons stored in a microwave superconducting cavity. The meters are circular Rydberg atoms, nonresonant with the cavity field. Their quantized light shift is measured by an atomic Ramsey interferometer (RI). We leave constant the system-meter interaction and adapt in real time the RI phase (i.e., the measured meter observable) to maximize information provided by each atomic detection. We demonstrate significant speedup in comparison with the previous "passive" photon counting method.

The experimental scheme is presented in Fig. 1 and described in detail in Refs. [13,14]. The high-Q microwave cavity C, resonant at $\omega_c/2\pi = 51.1$ GHz, is made of two superconducting Niobium mirrors separated by 2.8 cm and cooled down to 0.8 K (mean number of black-body photons 0.05) [15]. The photon lifetime is 65 ms. A microwave source S is used to inject a few-photon coherent field $|\alpha\rangle$ into C by diffracting radiation off the mirrors' edges. Its photon-number distribution $P_{\rm coh}(n)$ is Poissonian with average photon number $n_{\rm coh} = |\alpha|^2$.

Circular Rydberg atoms, excited in B from a Rubidium thermal beam, are used as meters. The atomic transition frequency $\omega_a/2\pi$ between levels $|g\rangle$ et $|e\rangle$ (principal quantum numbers 50 and 51, respectively) is detuned by $\delta/2\pi = 238$ kHz from $\omega_c/2\pi$. Being much larger than the the vacuum Rabi frequency $\Omega_0/2\pi = 47$ kHz, this

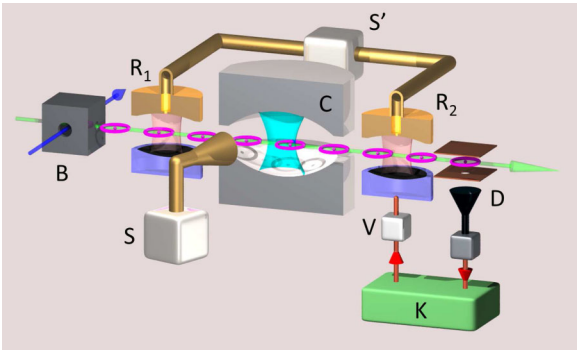

FIG. 1 (color online). Scheme of the experimental setup. Circular Rydberg atoms, prepared in box B, are detected in detector D at the exit of the Ramsey interferometer R_1–R_2 sandwiching the superconducting cavity C. As a function of the detection results, the controller K updates in real time its estimation of the actual photon-number distribution in C. It then chooses the optimal RI phase for the next atomic sample crossing R_2 by adjusting the potential V.

detuning precludes photon absorption or emission and enforces the QND nature of the measurement. Samples of atoms in state $|g\rangle$, propagating at a velocity $v = 250$ m/s, are prepared in B every $T_a = 83$ μs. The atom number in a sample obeys a Poisson statistics. The average number of atoms detected by state-selective field ionization in the detector D is $n_a = 0.35$.

The nonresonant atomic transition is light-shifted in setup C. This shift is measured by the RI, composed of the auxiliary cavities R_1 and R_2 fed by the source S′ and sandwiching C. A resonant $\pi/2$ pulse in R_1 prepares the coherent superposition $(|g\rangle - |e\rangle)/\sqrt{2}$. The dispersive atom-cavity interaction results in a phase shift $\varphi(n) \approx n\varphi_0$ of this atomic superposition. The phase shift per photon is $\varphi_0 = \Omega_0^2 t_{\rm eff}/2\delta$, where $t_{\rm eff}$ is the effective interaction time determined by v. In order to distinguish values of n from 0 to 7, we set $\varphi_0 \approx \pi/4$. A precise calibration provides $\varphi(n) = 0.255\pi n - 0.0015\pi n^2$, see [16] for the procedure and Fig. 2(a). The RI is completed by a $\pi/2$ pulse in R_2 after the atom has left C.

The conditional probability to detect finally an atom in state $s \in \{g, e\}$ is

$$P(s|\phi, n) = \{1 + jA + jB\sin[\varphi(n) - \phi]\}/2, \qquad (1)$$

where $j = 1$ (-1) for $s = g(e)$. The measured offset and contrast are $A = 0.008$ and $B = 0.685$. The RI phase ϕ is controlled via a transient Stark shift of ω_a produced by a voltage pulse V applied across R_2 (0.7 V for a π phase shift).

For a passive QND counting, with $n \in \{0\ldots7\}$, four settings of the RI phase, ϕ_i $(0 \le i \le 3)$, differing by about $\pi/4$ [dashed lines in Fig. 2(a)] are alternatively used in a preset way for successive atomic samples [5]. The detection probabilities $P(g|\phi_i, n)$ are plotted in Fig. 2(b). The setting

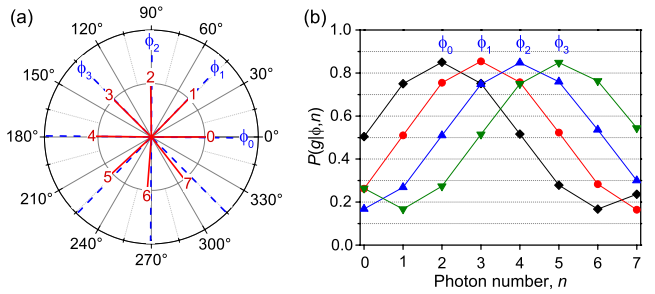

FIG. 2 (color online). Experimental phase settings. (a) Calibrated phase shifts $\varphi(n)$ for $n = 0$ to 7 (solid red lines) and the set of four RI phases ϕ_i (dashed blue axes). (b) Conditional probabilities $P(g|\phi, n)$ corresponding to the four ϕ_i's.

ϕ_i provides $P(g|\phi_i, n) \approx 0.5$ for $n = i$ and $n = i + 4$ and hence a maximum sensitivity of the signal to a change in n around these two numbers.

The photon-number distribution $P_k(n)$ after the detection of the kth atom is deduced from $P_{k-1}(n)$ by Bayes' law. If the atom is found in state s_k using phase ϕ_{p_k} with $p_k = 0\ldots3$, the distribution $P_k(n)$ is

$$P_k(n) = P_{k-1}(n)P(s_k|\phi_{p_k}, n)/P(s_k|\phi_{p_k}), \qquad (2)$$

with $P(s_k|\phi_{p_k}) = \sum_n P_{k-1}(n)P(s_k|\phi_{p_k}, n)$. The multiplication of $P_{k-1}(n)$ by $P(s_k|\phi_{p_k}, n)$ enhances the probabilities of photon numbers most compatible with the detected state s_k and reduces those of photon numbers least compatible. Many successive detections decimate n until a single random $n_{\rm cov}$ is left [5,17]. This process requires on the average 70 atomic detections to converge to $P(n_{\rm cov}) > 0.8$. This passive method has been used for preparing Fock states [16,18] and for field sensing in quantum feedback loops locking n in spite of decoherence [19,20].

Our adaptive measurement process notably increases the information flux by actively adjusting, in real time, the RI phase ϕ for each atomic sample. We quantify the information in $P(n)$ by the normalized Shannon entropy,

$$S(P(n)) = \frac{1}{\ln(1/8)} \sum_{n=0}^{7} P(n)\ln P(n). \qquad (3)$$

The limiting entropy values 0 and 1 correspond to a pure number state and to a uniform distribution $P_{\rm uni}(n) = 1/8$, respectively.

After detecting the kth atom, the real-time controller K (Fig. 1) calculates $P_k(n)$ from $P_{k-1}(n)$. Then, for each possible choice of RI phase to be applied to the next sample entering R_2, K evaluates the statistical average of S over the two possible atomic detections. The phase leading to the largest entropy reduction is then implemented. Due to the spatial separation of R_2 and D (86 mm), the chosen phase is applied to the $(k + 4)$th sample. Since the atom-field interaction is QND, the three not-yet-detected samples

do not modify $P(n)$ and thus are not considered in making the decision.

In a first experiment, we demonstrate the gain of the adaptive measurement of a field in a well defined photon-number state. We use a three-section experimental sequence starting by the injection of a 3.5-photon coherent field. In the first section we perform a state preparation using a passive QND photon number counting. In the second section we run the adaptive sequence. In the last section we perform a state verification with a second passive counting. We postselect for analysis only those sequences for which the photon counts in the passive sections, n_{ini} and n_{fin}, are the same. In this way, we eliminate photon number jumps and operate with an effectively relaxation-free system.

The passive sections use the procedure described in [18]. In addition to the Bayesian estimation of $P_k(n)$, it takes into account the small evolution of $P(n)$ between successive samples due to field relaxation [13,16]. The state preparation section starts with $P_0(n) = P_{\mathrm{coh}}(n)$. The controller stops it when one of the photon-number probabilities, $P_k(n_{\mathrm{ini}})$, reaches 0.8. The verification section starts with $P_0(n)$, peaked at n_{ini}, modeling the state at the end of the first section and including a calculated relaxation process during the 25-ms-long (300 atomic samples) intermediate adaptive measurement. The verification stops when the probability of any n_{fin} reaches 0.8.

For a fair estimation of the adaptive section performance, we do not assume any *a priori* knowledge on the field and start the decimation with $P_0(n) = P_{\mathrm{uni}}(n)$. For the first four samples (no atomic detection yet), we preset the detection phase. Then, we choose it according to the entropy optimization algorithm. We analyze the measurement performance using all postselected data, for all n_{ini} values. We define, for each sequence, a distribution of relative photon numbers, $P'_k(\Delta n) = P_k(n = (n_{\mathrm{ini}} + \Delta n) \bmod 8)$ with $\Delta n = ((n - n_{\mathrm{ini}} + 3) \bmod 8) - 3$. The relative photon number Δn is thus equal to 0 for $n = n_{\mathrm{ini}}$ and is limited to $-3 \le \Delta n \le 4$.

We have realized 19500 sequences and postselected about 6000 of them. Figure 3(a) shows the relative distribution $\overline{P'_k}(\Delta n)$ averaged over all postselected sequences. Starting from the flat distribution, $\overline{P'_k}(0)$ monotonically increases to ≈ 0.8. The neighboring probabilities, $\overline{P'_k}(\pm 1)$, first increase (initial squeezing of $P(n)$ around n_{ini}), and then asymptotically decrease to ≈ 0.1. The probabilities of other photon numbers monotonically decrease towards 0.

In order to assess the adaptive measurement speedup, we perform a control experiment in which the central section of the sequence is replaced by a simple passive measurement with preset RI phases. The photon number decimation procedure is identical to that of the adaptive section. The dashed line in Fig. 3(a) presents the time evolution of $\overline{P'_k}(0)$ for about 6200 postselected passive measurements. The asymptotic value is nearly the same as in the adaptive case, but the convergence is slower.

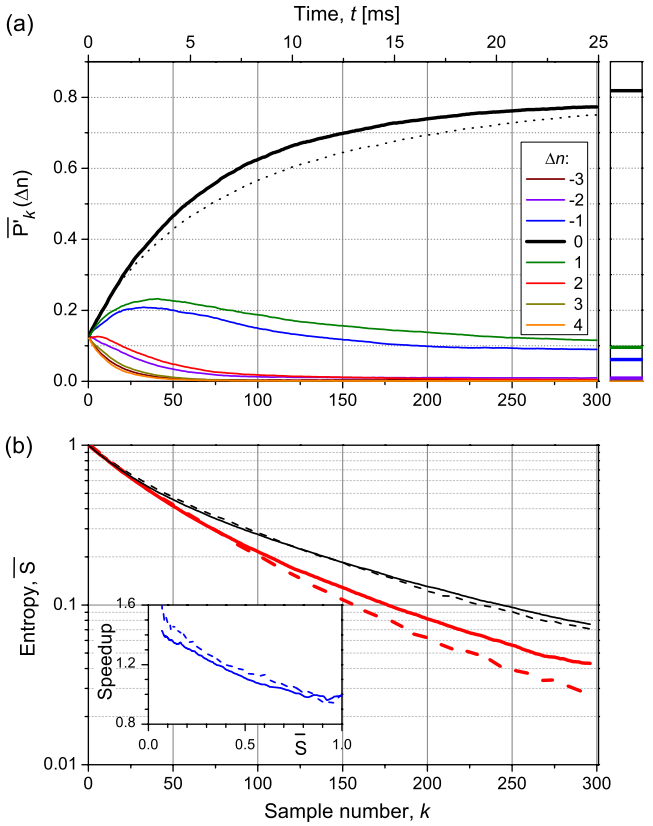

FIG. 3 (color online). Adaptive measurement of a nondecaying field. (a) Average evolution of the relative photon-number distribution $\overline{P'_k}(\Delta n)$. The right bar displays the values of the reconstructed $\overline{P'_{\mathrm{ML}}}(\Delta n)$, averaged over all n_{ini}. (b) Average entropy for passive (black thin line) and adaptive (red thick line) measurements. Solid and dashed lines are experimental and simulation results, respectively. Inset: speedup of information acquisition when using the adaptive measurement.

The asymptotic value of $\overline{P'_k}(0) < 1$ could be either due to an imperfection in the adaptive procedure itself or to an imperfect state selection by the passive sections of the sequence. We thus assess the purity of states postselected with n_{ini} by performing a maximum-likelihood (ML) reconstruction of the photon-number distribution $P_{\mathrm{ML}}(n)$ on the ensemble of all sequences assigned to this n_{ini} value [21]. The reconstruction is based upon the analysis of all atomic detections in the passive central sections of these sequences. We then compute the relative photon-number distribution averaged over all n_{ini}, $\overline{P'_{\mathrm{ML}}}(\Delta n)$, shown in the right bar in Fig. 3(a). It is in fair agreement with the asymptotical values of $\overline{P'_k}(\Delta n)$. The reduced value of $\bar{P}'_k(0)$ is thus mostly due to the imperfect state selection.

To get a better insight into the data acquisition rate, we plot in Fig. 3(b) the evolution of the entropy $\bar{S}$ averaged over all adaptive (solid thick black line) and passive (solid thin red line) postselected sequences. The inset in Fig. 3(b) presents a speedup factor defined as the ratio of the measurement times needed to reach, on the average, the

same entropy with each method. With the adaptive measurement, we reach $\bar{S} = 0.2$ (corresponding to a 90% confidence in one n value) about 25% faster. The speedup is even larger for smaller entropies. The dashed lines in Fig. 3(b) indicate the results of Monte Carlo simulations. The agreement with the experiment is good in the initial phase of the decimation process, down to $\bar{S} \approx 0.1$. The discrepancies, mainly noticeable for low entropies, are due to the slow drift of the RI phase during the one-hour duration of the experiment.

We have also studied the probability distribution of the RI phase choice. We have observed that K, after a few detections, preferably chooses, with an ≈50% probability, a midfringe phase setting for the most likely photon number. The orthogonal phase, less sensitive to this photon number, is seldom chosen.

In a second experiment we use the adaptive measurement concept to speed up the preparation of a Fock state out of an initial coherent field. We compare the passive state preparation described above (first section of the sequence) to an active scheme, which takes into account the known initial coherent photon-number distribution and cavity relaxation. As above, the controller stops the state preparation sequence as soon as one of the photon-number probabilities reaches 0.8. The sequence is repeated 9000 times. We check, for each converged photon number n_{cov}, the final state of the field by performing ML reconstruction of its photon-number distribution $P_{\mathrm{ML}}(n)$. For this procedure we use data provided by 400 passive measurement samples sent after each state preparation sequence. Within a few percent, the average $P(n)$ provided by K after convergence to n_{cov} is equal to $P_{\mathrm{ML}}(n)$.

In order to evaluate the reduction of the convergence time due to the measurement adaptation, we calculate and plot in Fig. 4 the fraction $\eta(t)$ of sequences having converged before time t for adaptive (black thin line) and passive (red thick line) measurements. These curves include all data independently of n_{cov}. Half of the adaptive sequences converge within 6.9 ms, whereas 10 ms, i.e., 45% more time, are required for the passive method. The inset in Fig. 4 shows the ratio of the times required to reach the same η value in the active and passive methods. Note that the ratio of entropies reached in the active and passive methods does not provide a fair measurement of the speedup factor, as it was the case for Fig. 3(b), since all adaptive measurements are stopped at $P(n_{\mathrm{cov}}) = 0.8$, corresponding to $S \approx 0.3$.

In conclusion, we have implemented an adaptive projective QND measurement applied to the photon number states of a field stored in a cavity. It relies on the real-time choice of the atomic meter measurement basis optimizing the acquisition of information on the system. We have compared the performance of this method to that of the passive measurement procedure based on a randomly chosen measurement basis. The adaptive method is shown

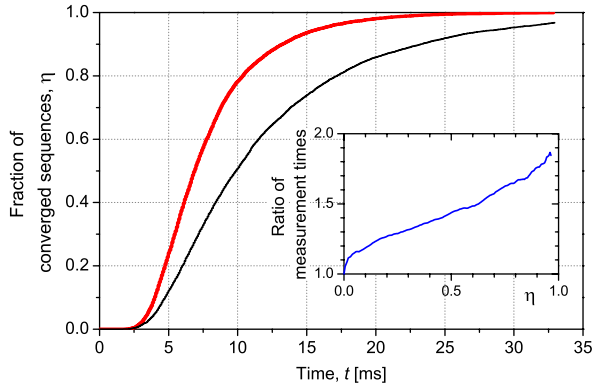

FIG. 4 (color online). Adaptive preparation of photon number states. The fraction η of converged sequences for passive (black thin line) and adaptive (red thick line) measurements is plotted versus measurement time t. Inset: Ratio of passive to adaptive measurement time necessary to reach a given η.

to provide a significant speedup of information acquisition and a large reduction of the resources (atoms) required. This is essential for extending the measurement to higher, thus faster decaying, photon number states. Since their lifetime scales inversely with their size, the ξ-fold shortening of the measurement time straightway increases the maximal measurable photon number by $1/\xi$, making thus possible the study of quantum states not accessible with standard passive probing. For instance, this method would increase the bandwidth of a quantum feedback loop preparing and stabilizing photon number states of light [22] and allow us the stabilization of shorter-lived states.

This experiment adapts the measurements performed on the meter while keeping its interaction with the system unchanged. The natural extension of this method is to set also in real time the parameters of this interaction. As was shown in [23], this strategy allows one to reach ideally the limit set by information theory according to which N atoms are enough for counting up to $2^N - 1$ photons. Numerical simulations show that a logarithmic dependence of the number of required resources on the quantum system's size can be reached even in the presence of realistic imperfections.

The authors acknowledge support from the European Research Council (DECLIC project), the European Community (SIQS project), and the Agence Nationale de la Recherche (QUSCO-INCA project).

*igor.dotsenko@lkb.ens.fr

[1] V. B. Braginsky and F. Y. Khalili *Quantum Measurement* (Cambridge University Press, Cambridge, England, 1999).
[2] C. M. Caves, in *Quantum Optics, Experimental Gravity, and Measurement Theory*, edited by P. Meystre and M. Scully, NATO Advanced Science Institutes Series Vol. 94, p. 567 (Springer, New York, 1983).

[3] P. Grangier, J. A. Levenson, and J.-P. Poizat, Nature (London) **396**, 537 (1998).
[4] J. Appel, P. J. Windpassinger, D. Oblak, U. Hoff, N. Kjaergaard, and E. S. Polzik, Proc. Natl. Acad. Sci. U.S.A. **106**, 10960 (2009).
[5] C. Guerlin, J. Bernu, S. Deléglise, C. Sayrin, S. Gleyzes, S. Kuhr, M. Brune, J.-M. Raimond, and S. Haroche, Nature (London) **448**, 889 (2007).
[6] H. M. Wiseman and G. J. Milburn, *Quantum Measurement and Control* (Cambridge University Press, Cambridge, England, 2009).
[7] M. A. Armen, J. K. Au, J. K. Stockton, A. C. Doherty, and H. Mabuchi, Phys. Rev. Lett. **89**, 133602 (2002).
[8] R. Okamoto, M. Iefuji, S. Oyama, K. Yamagata, H. Imai, A. Fujiwara, and S. Takeuchi, Phys. Rev. Lett. **109**, 130404 (2012).
[9] D. B. Hume, T. Rosenband, and D. J. Wineland, Phys. Rev. Lett. **99**, 120502 (2007).
[10] A. Serafini, ISRN Optics **2012**, 275016 (2012).
[11] B. R. Johnson *et al.*, Nat. Phys. **6**, 663 (2010).
[12] A. Reiserer, S. Ritter, and G. Rempe, Science **342**, 1349 (2013).
[13] S. Haroche and J. M. Raimond, *Exploring the Quantum: Atoms, Cavities and Photons* (Oxford University Press, New York, 2006).
[14] J.-M. Raimond, M. Brune, and S. Haroche, Rev. Mod. Phys. **73**, 565 (2001).
[15] S. Kuhr *et al.*, Appl. Phys. Lett. **90**, 164101 (2007).
[16] M. Brune, J. Bernu, C. Guerlin, S. Deléglise, C. Sayrin, S. Gleyzes, S. Kuhr, I. Dotsenko, J. Raimond, and S. Haroche, Phys. Rev. Lett. **101**, 240402 (2008).
[17] M. Bauer and D. Bernard, Phys. Rev. A **84**, 044103 (2011).
[18] S. Deléglise, I. Dotsenko, C. Sayrin, J. Bernu, M. Brune, J.-M. Raimond, and S. Haroche, Nature (London) **455**, 510 (2008).
[19] C. Sayrin *et al.*, Nature (London) **477**, 73 (2011).
[20] X. Zhou, I. Dotsenko, B. Peaudecerf, T. Rybarczyk, C. Sayrin, S. Gleyzes, J. M. Raimond, M. Brune, and S. Haroche, Phys. Rev. Lett. **108**, 243602 (2012).
[21] C. Sayrin, I. Dotsenko, S. Gleyzes, M. Brune, J. M. Raimond, and S. Haroche, New J. Phys. **14**, 115007 (2012).
[22] B. Peaudecerf, C. Sayrin, X. Zhou, T. Rybarczyk, S. Gleyzes, I. Dotsenko, J. M. Raimond, M. Brune, and S. Haroche, Phys. Rev. A **87**, 042320 (2013).
[23] S. Haroche, M. Brune, and J. M. Raimond, J. Phys. II (France) **2**, 659 (1992).